Optical/X-ray variations of the changing-look AGN IRAS 23226-3843

W. Kollatschny

D. Grupe, M.L. Parker, M.W. Ochmann, N. Schartel,
E. Romero-Colmenero, H. Winkler. S. Komossa,
P. Famula, M.A. Probst, M. Santos-Lleo

2023, A&A 670, A103

Napoli, 2023

IRAS 23226-3843

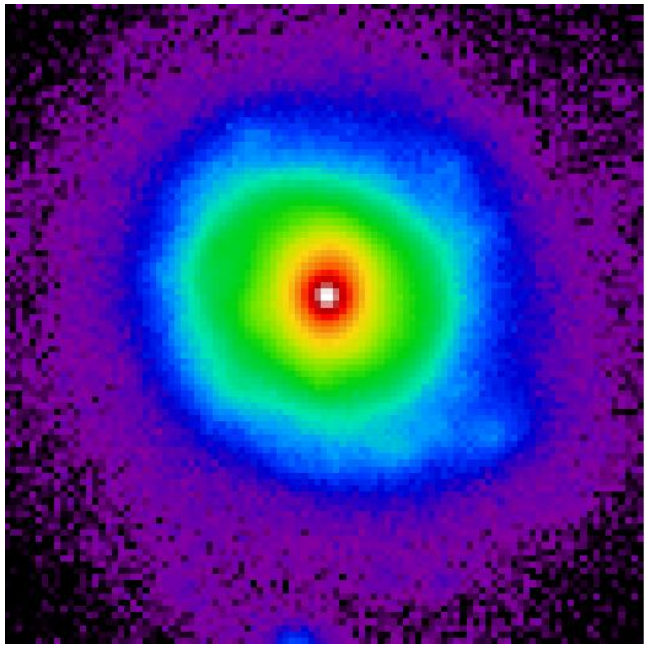

DESI legacy image (r band),
scale: 0.44 x 0.44 arcmin =
18.1 x 18.1 kpc

SED:radio, FIR, opt., X-ray

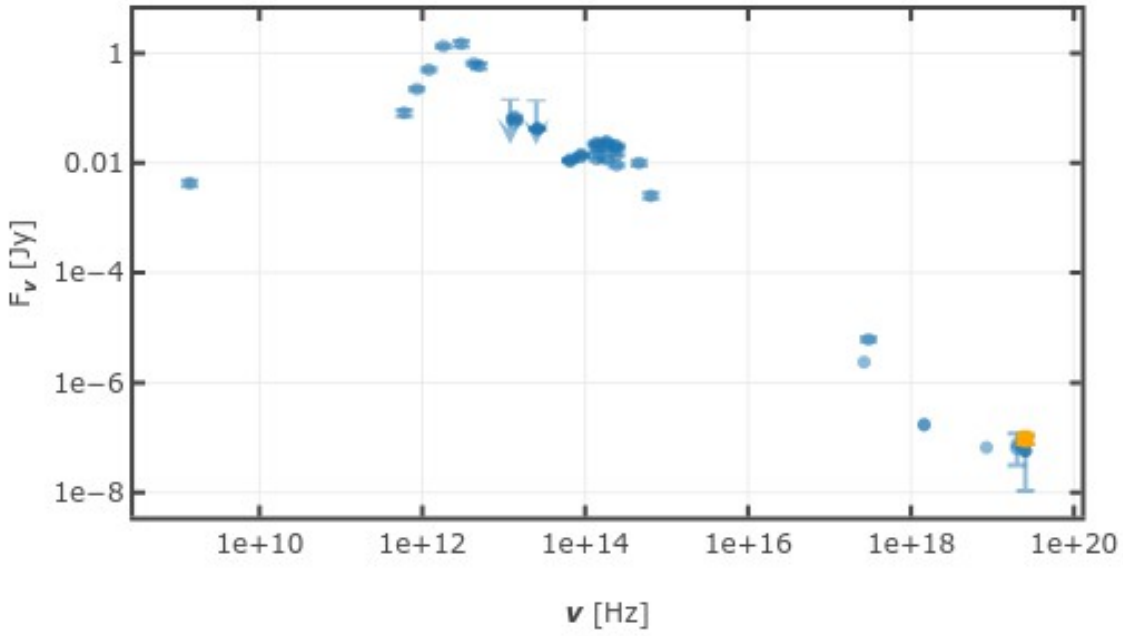

listed in IRAS Faint Source catalogue

- S0 type, z = 0.036
- m_v ~ 13.7, M_v = - 22.3

IRAS 23226-3843

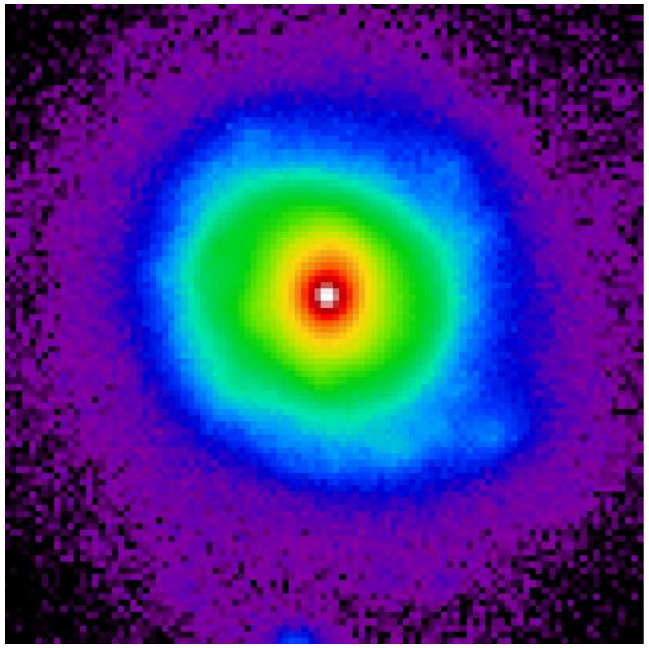

DESI legacy image (r band),
scale: 0.44 x 0.44 arcmin =
18.1 x 18.1 kpc

- S0 type, z = 0.036
- m_v ~ 13.7, M_v = - 22.3

XMM slew survey:
- decline in X-ray (May 2017)
by factor of 10,
in comparison to ROSAT 1990

- opt. spectroscopy with: SALT
- spectral types (1999→ 2017):

broad line Sy1 →Sy1.9

Opt./UV/X-ray broad band var. in IRAS23226-3843

2007 2017

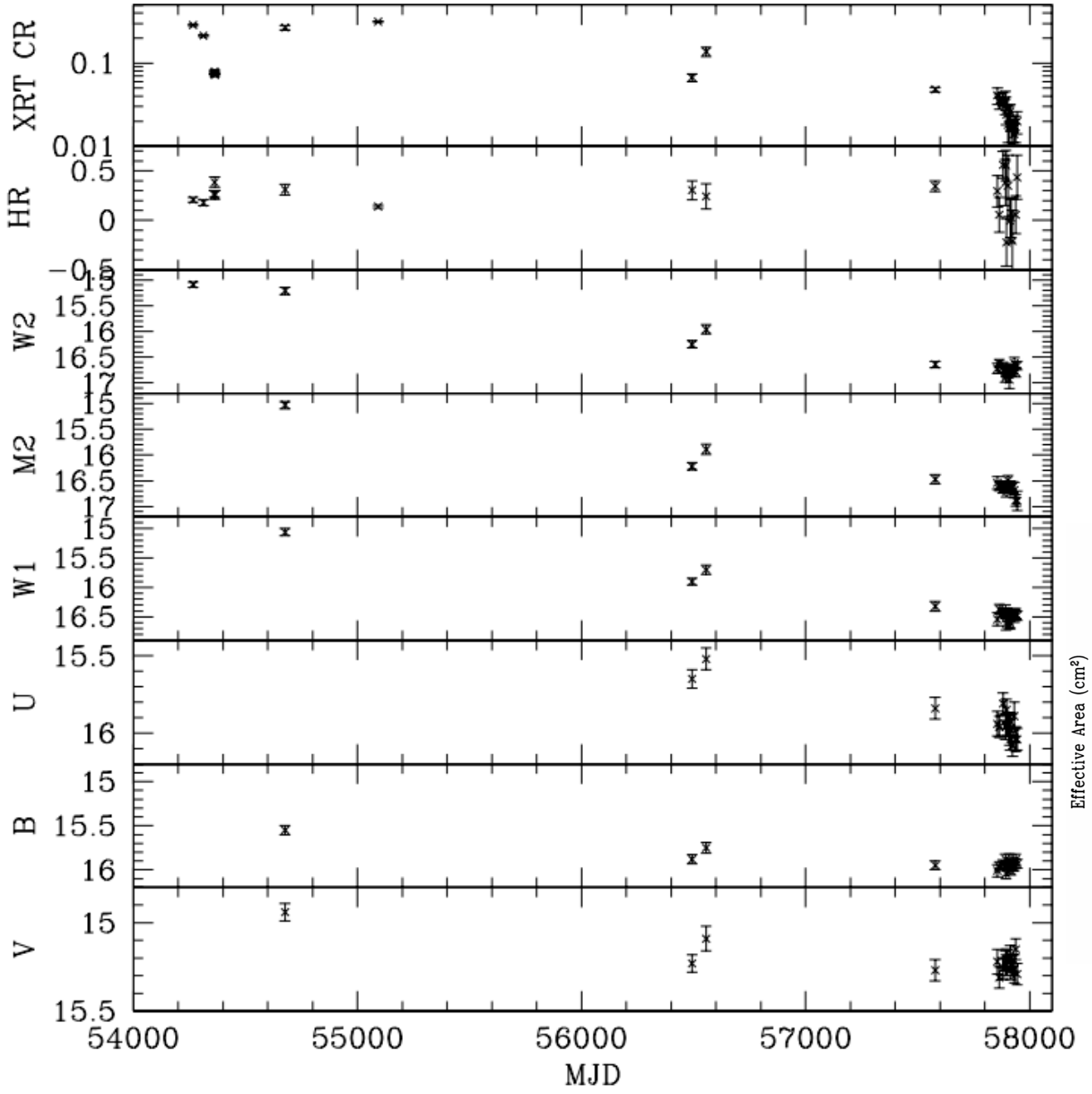

decrease:

X-ray: factor >10

Swift: 2007 - 2017

opt.: factor 2

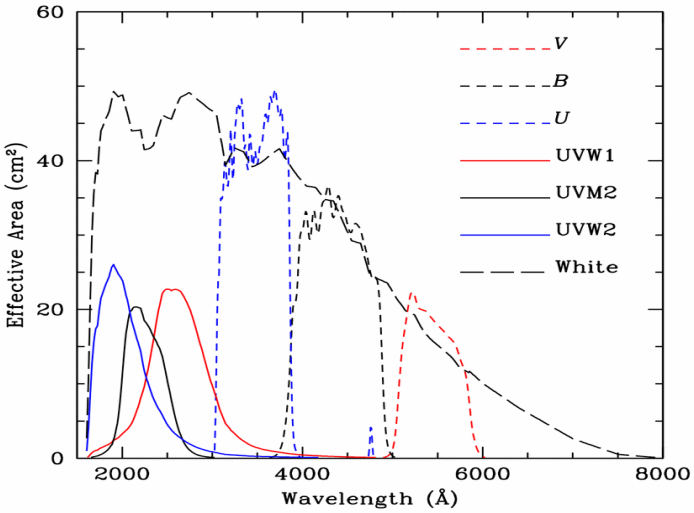

Optical spectral variations in IRAS23226-3843

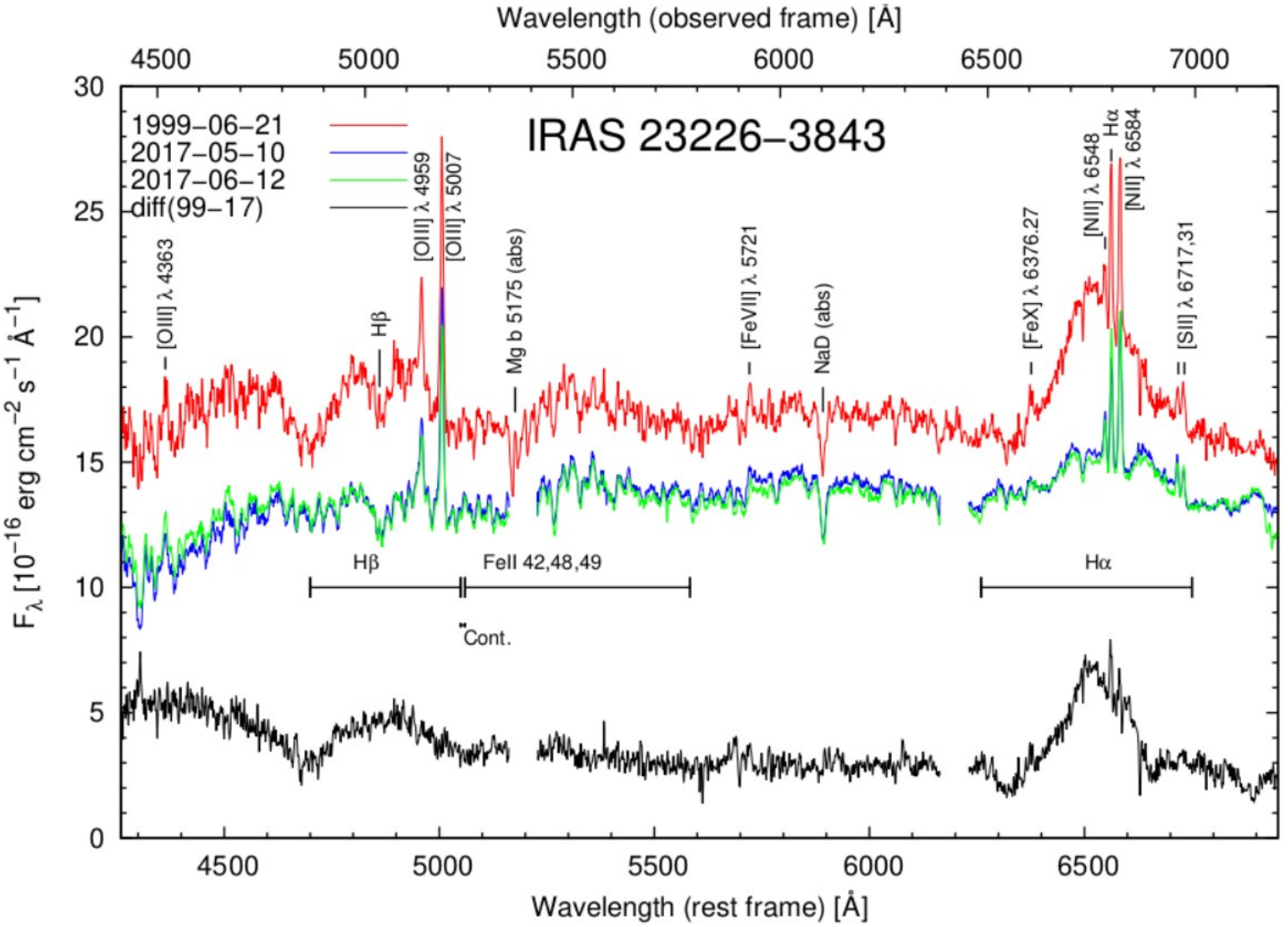

spectral *types (1999→ 2017):* **Sy1 → *Sy1.9***

Combined X-ray, UV, and optical light curves taken with Swift for the years 2007 until 2021. The fluxes are given in units of 10^-12 ergs s^-1 cm^-2. HR is the X-ray hardness ratio. The red lines indicate the dates of our deep XMM observations. The observations for the year 2019 (shaded area) are presented in greater detail in next Figure.

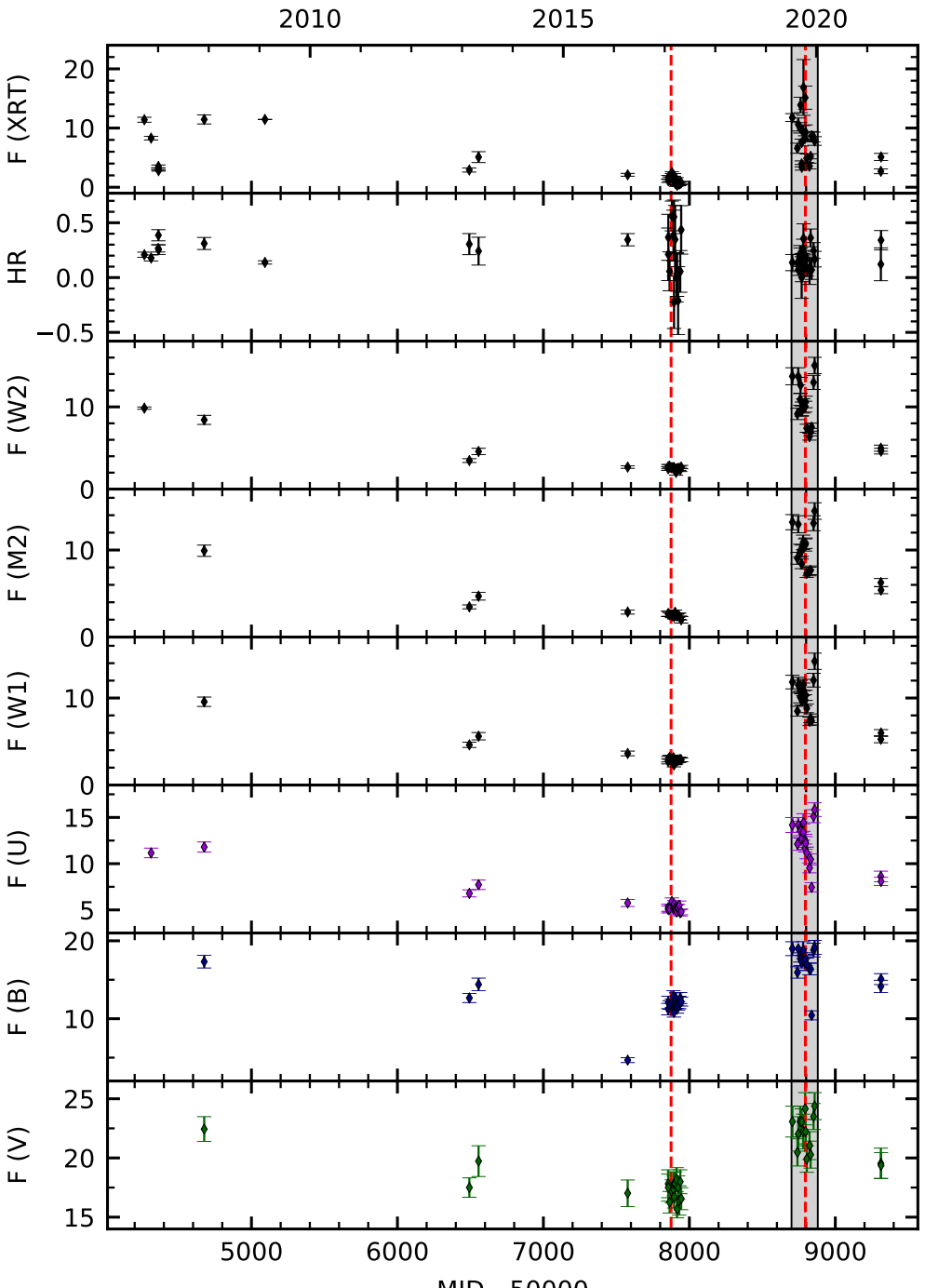

August 2019 : strong X-ray outburst detected with Swift

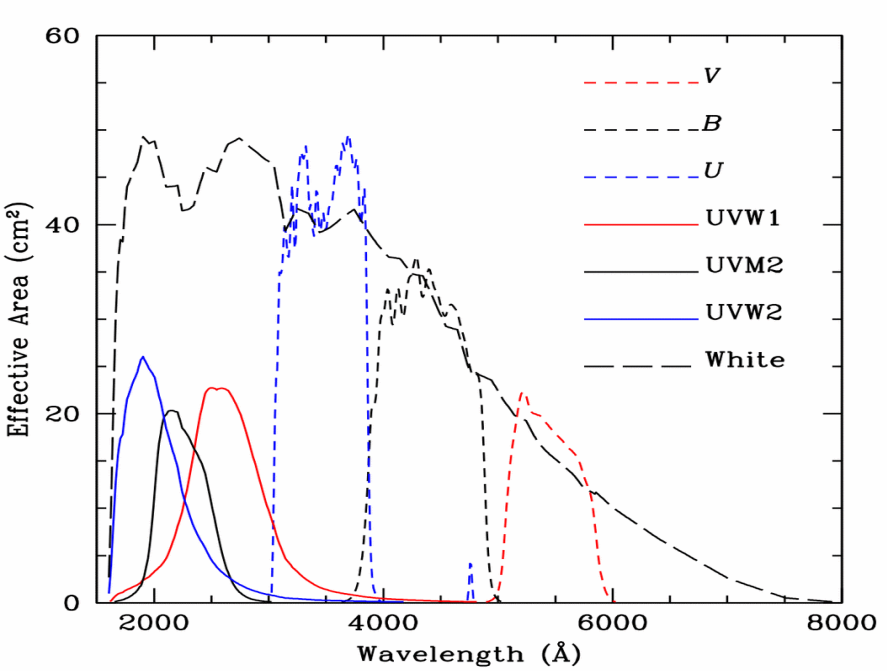

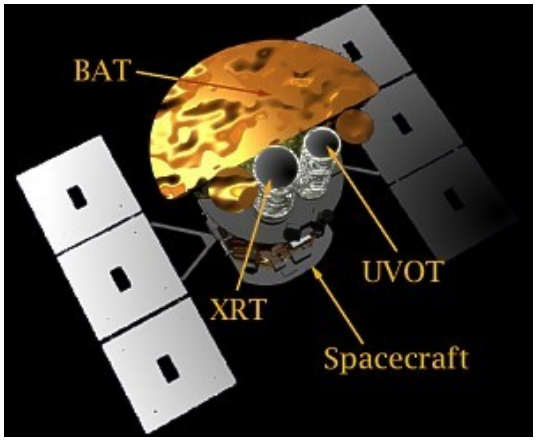

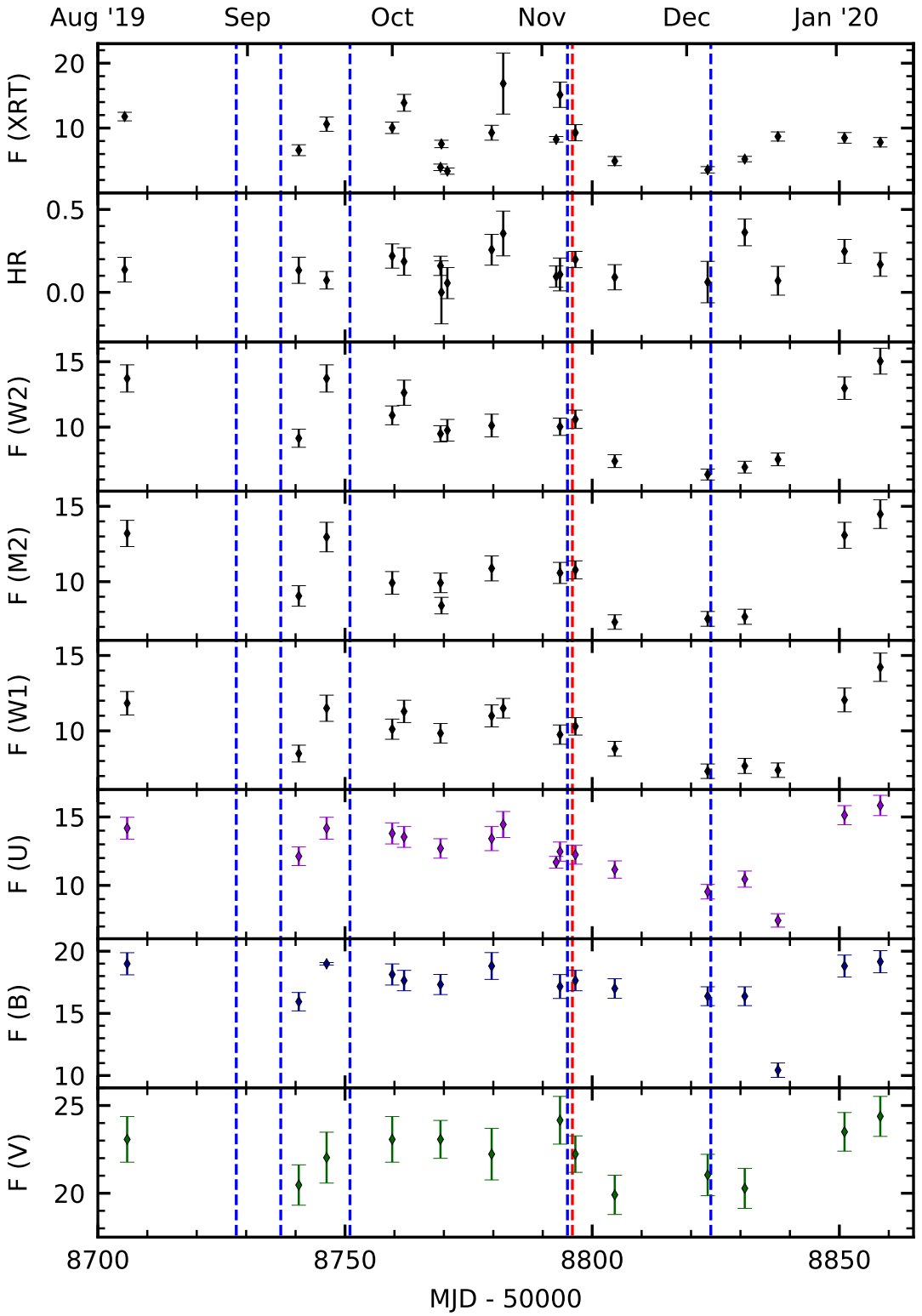

Combined X-ray, UV, and optical light curves taken with Swift for the year 2019.

The fluxes are given in units of 10^-12 ergs s-1 cm^-2.

Furthermore, the dates of our optical spectral observations are indicated as blue lines.

We note that the deep XMM observation was performed on MJD 58795 (red line).

Hardness ratio (HR) of our Swift observations as a function of X-ray flux (2007-2021): there is **no systematic trend** of HR with flux.

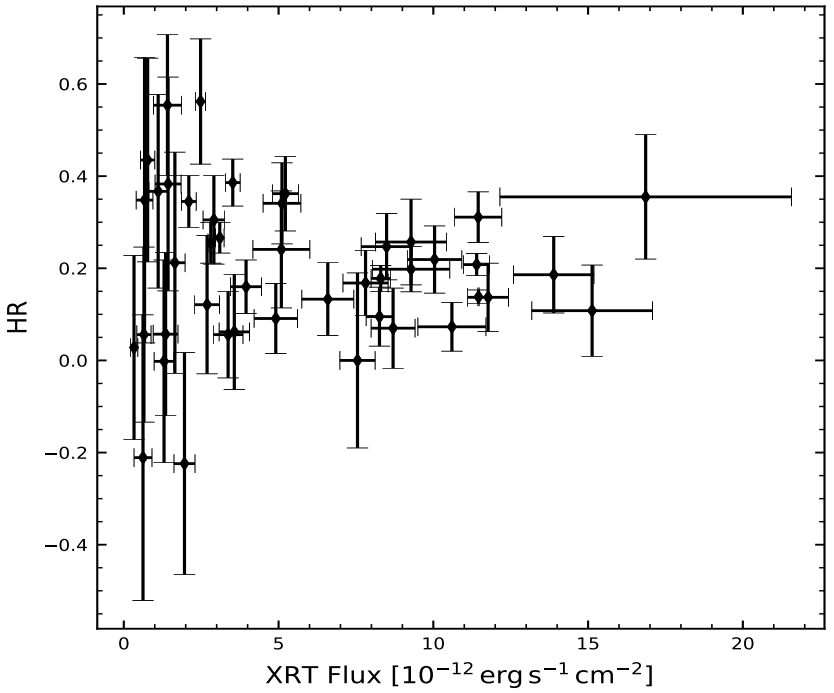

<u>Comparison of the broadband X-ray data in 2017 and 2019</u>

The change in flux is a uniform increase of a factor of ~10 across the bandpass, and both spectra show residuals in the Fe K band. The gray line shows the 2017 data scaled up by a factor of 10 to match the 2019 data. Above ~3keV the agreement in spectral shape is very good, below 3 keV the 2019 data is relatively higher, with the difference increasing toward lower energies.

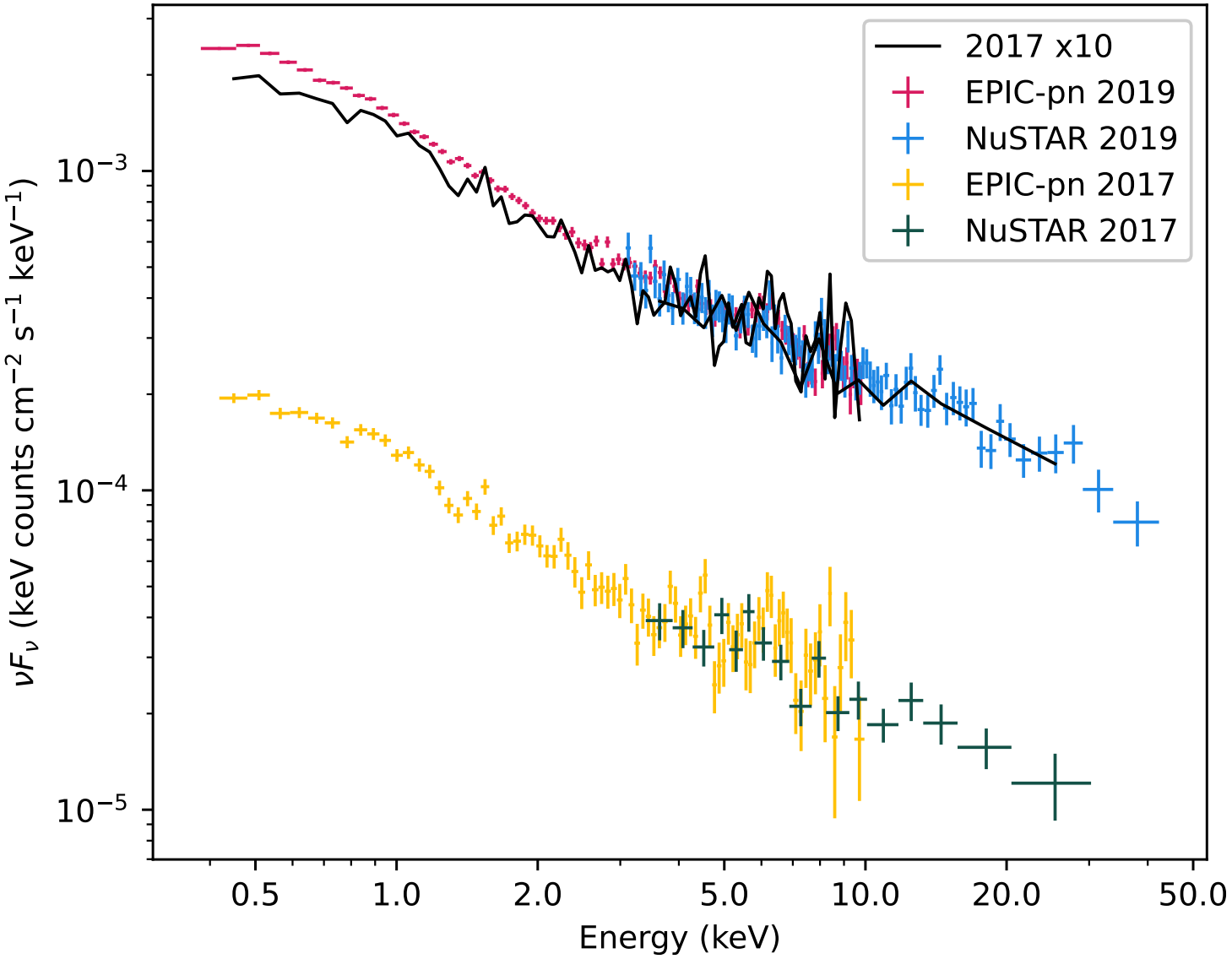

Ratio of the **XMM and NuSTAR spectra** to a power-law continuum and Comptonized soft excess model, in the Fe K band. A **moderately broadened emission line is visible, and a possible absorption feature is present between 7 and 8 keV** in the EPIC-pn spectrum. The NuSTAR data are consistent with both features, but are noisier.

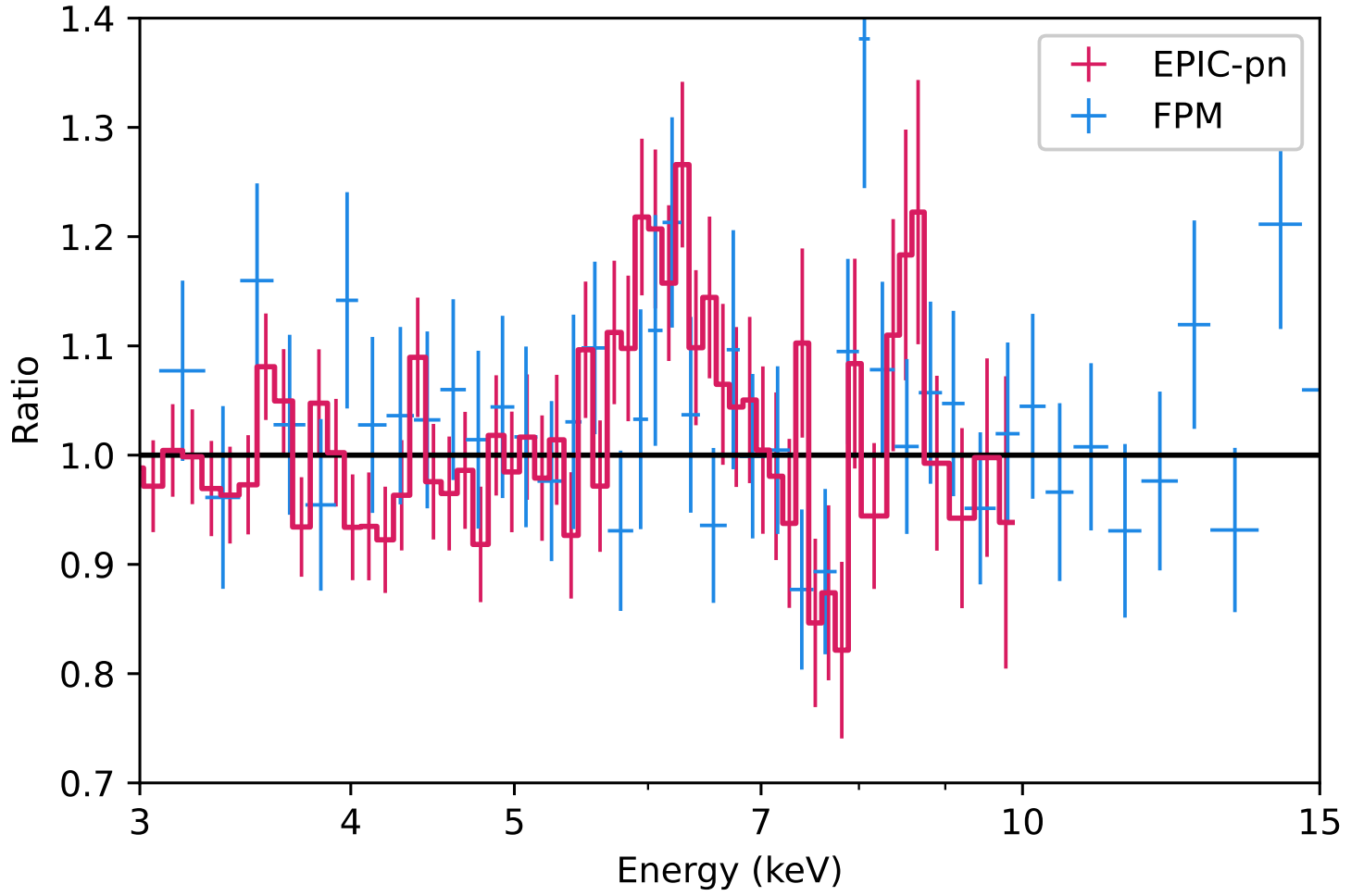

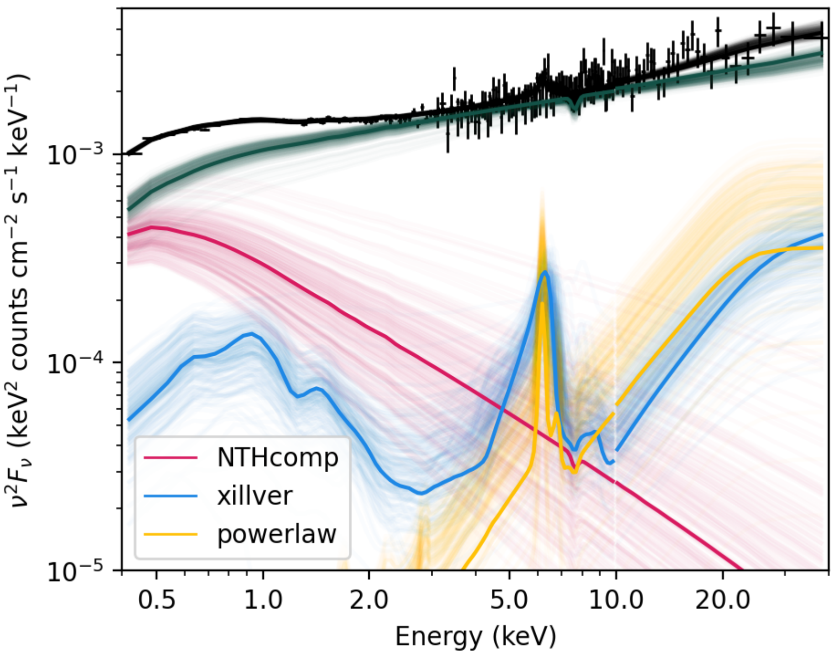

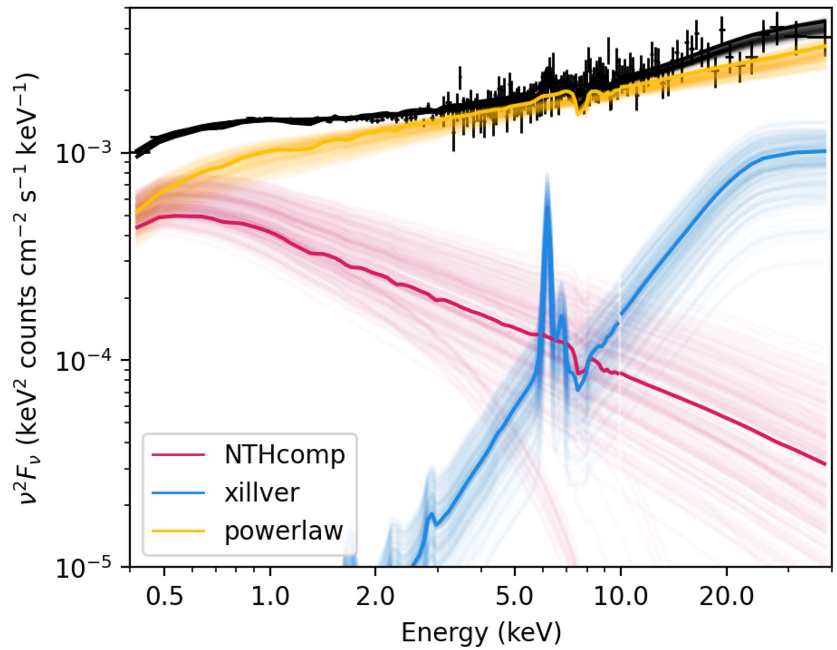

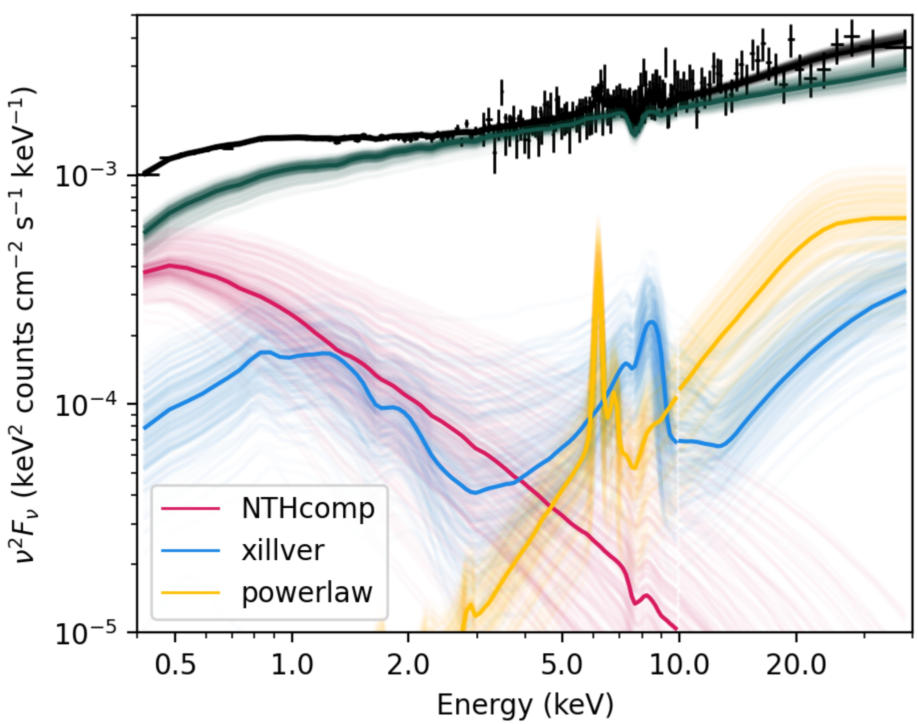

Model spectra for the three different X-ray models, fit to the 2019 XMM EPIC-pn spectrum. Top left shows the reflection model, top right the disk wind model, and bottom the hybrid model.

In each case, **the points with error bars show the data, and the black lines show the total model spectra.** For the disk wind and hybrid models, the disk wind component is included as a multiplicative component applied to all other spectra components apart from the distant reflection. In the reflection model we apply a Gaussian absorption line to all additive components aside from the distant reflection to account for the possible absorption feature.

(Michael Parker)

<u>Long-term light curves</u> of the continuum flux density at 5040 Å (in units of 10^-15 erg s^1 cm^-2 Å^-1, as well as of the line fluxes **of Hα, Hβ, and Fe II (42,48,49)** (in units 10^-15 erg s^-1,cm^-2) for the years **1997 until 2020**. The right panel shows, in addition to the observations from 2017 and 2020, the variations in **2019** in more detail. The epochs of the deep XMM observations are indicated by a red arrow.

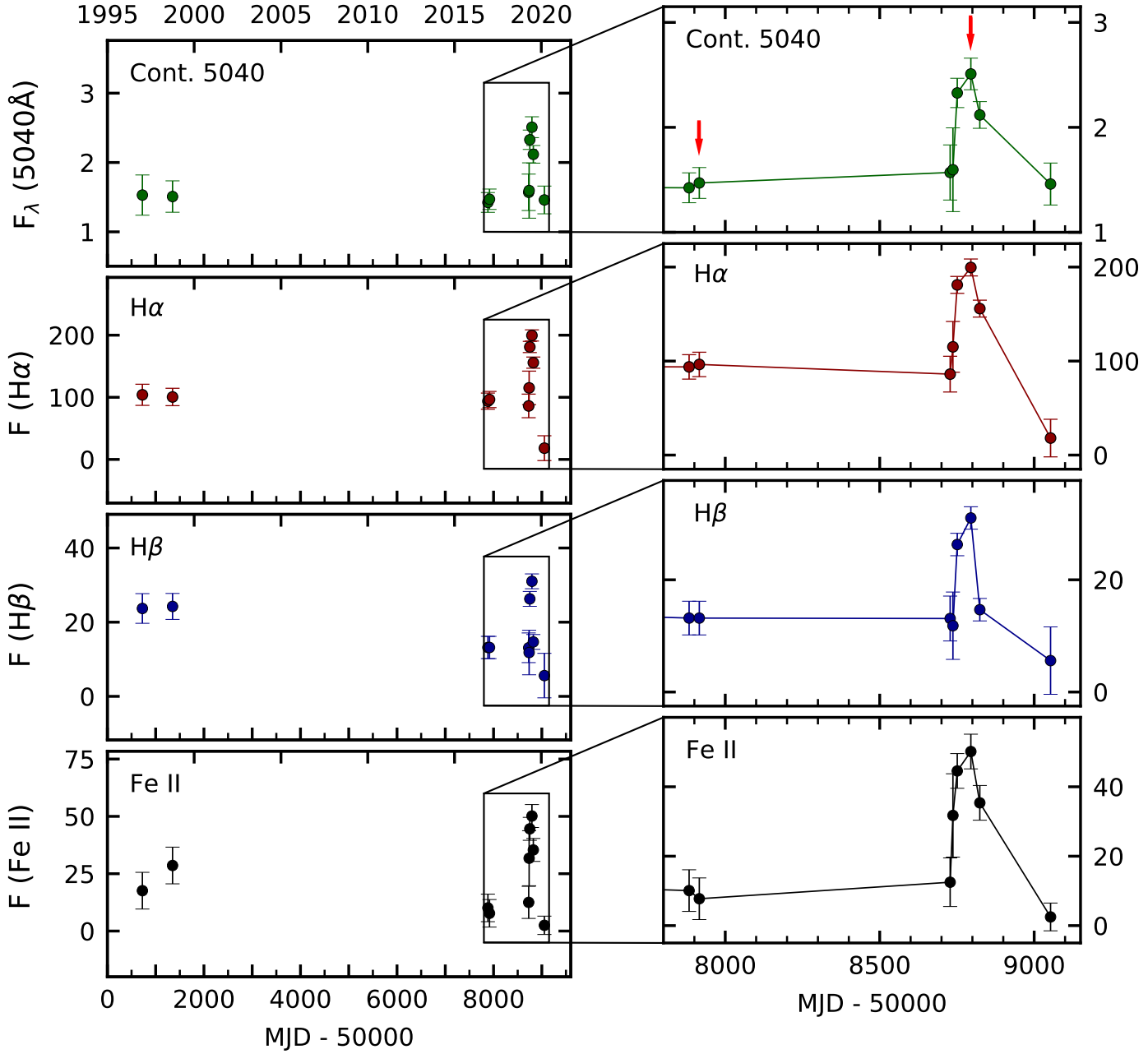

Optical spectra for the years 1997 until 2020.

The spectra were calibrated to the same absolute [OIII]λ5007 flux.
The three outburst spectra from 2019 are indicated by their observation date.

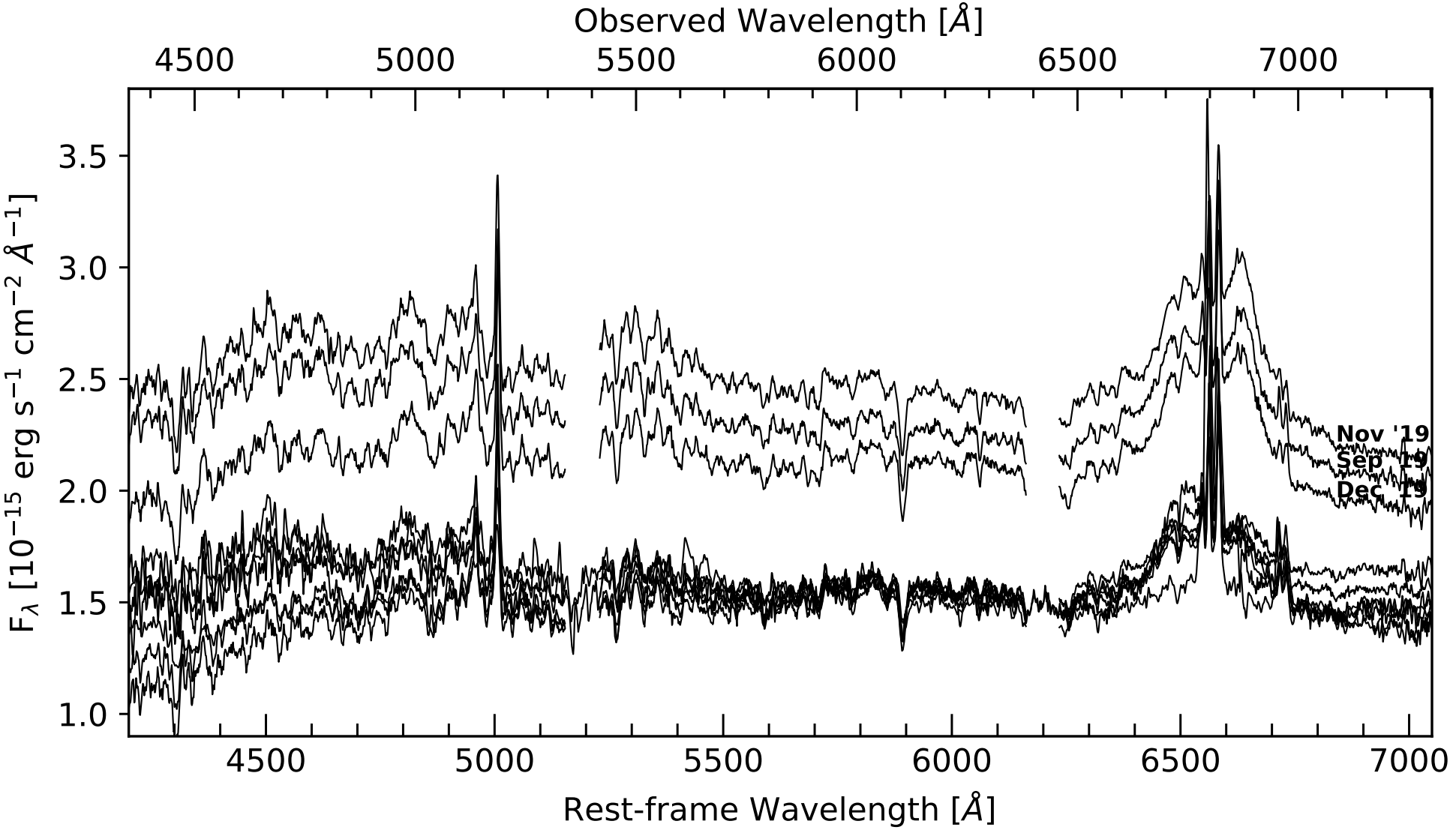

Mean (black) and rms (red) spectra of IRAS 23226-3843.
The rms spectrum has been scaled by a factor of 6.5 to enhance weaker line structures.
The Balmer lines Hα and Hβ as well as Fe II blends are indicated by black lines.

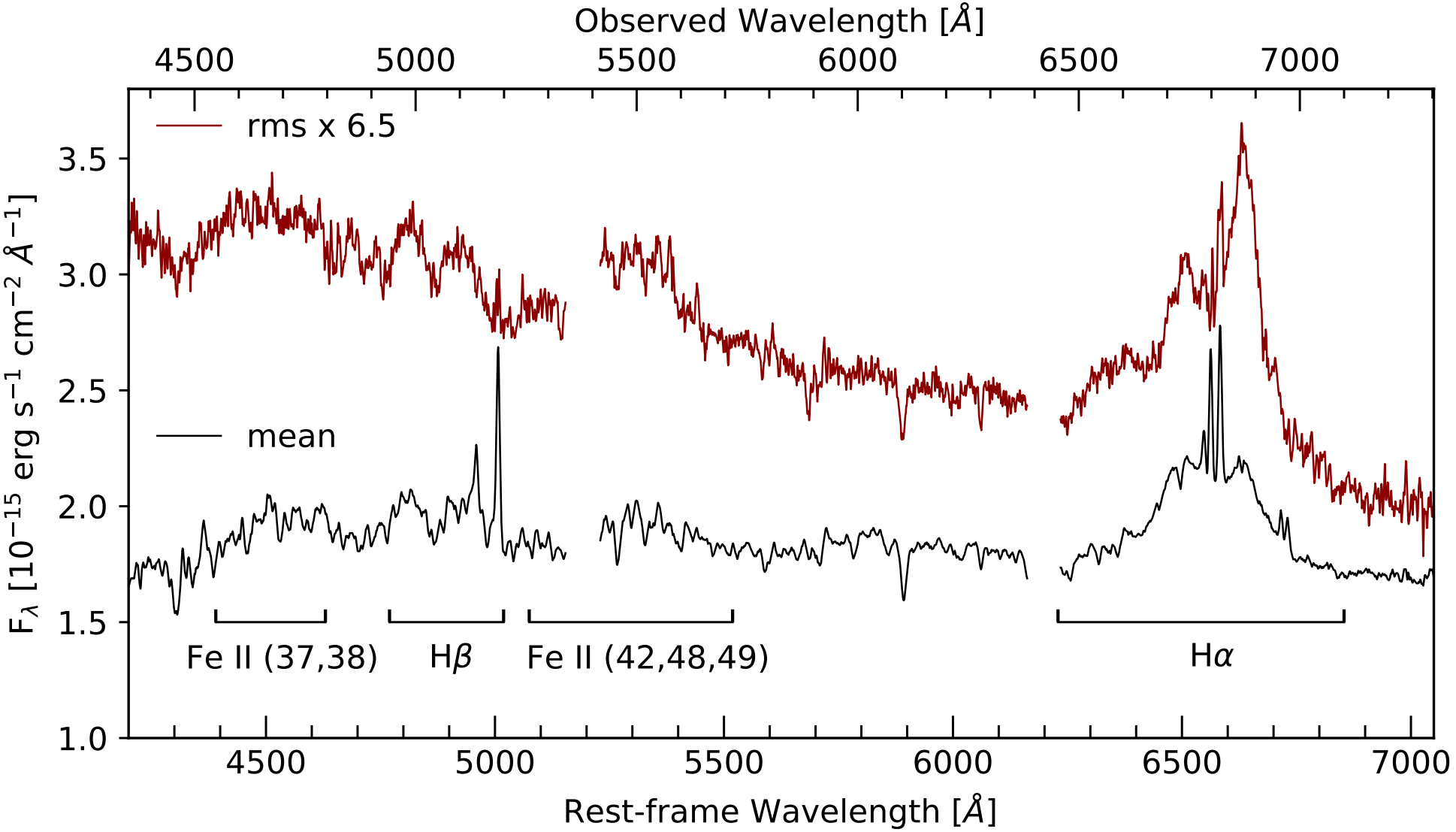

Observed spectrum taken on 2019 Sept 24 **(red)** and **synthesis fit** with pPXF (Cappellari 2017). The green line is the combined pPXF fit for the **stellar component (orange)** and the additional **power-law component (light blue).**
The **residuum spectrum (purple)** i.e., the difference between the observed spectrum and the combined pPXF fit, gives the clean **emission line contribution**.

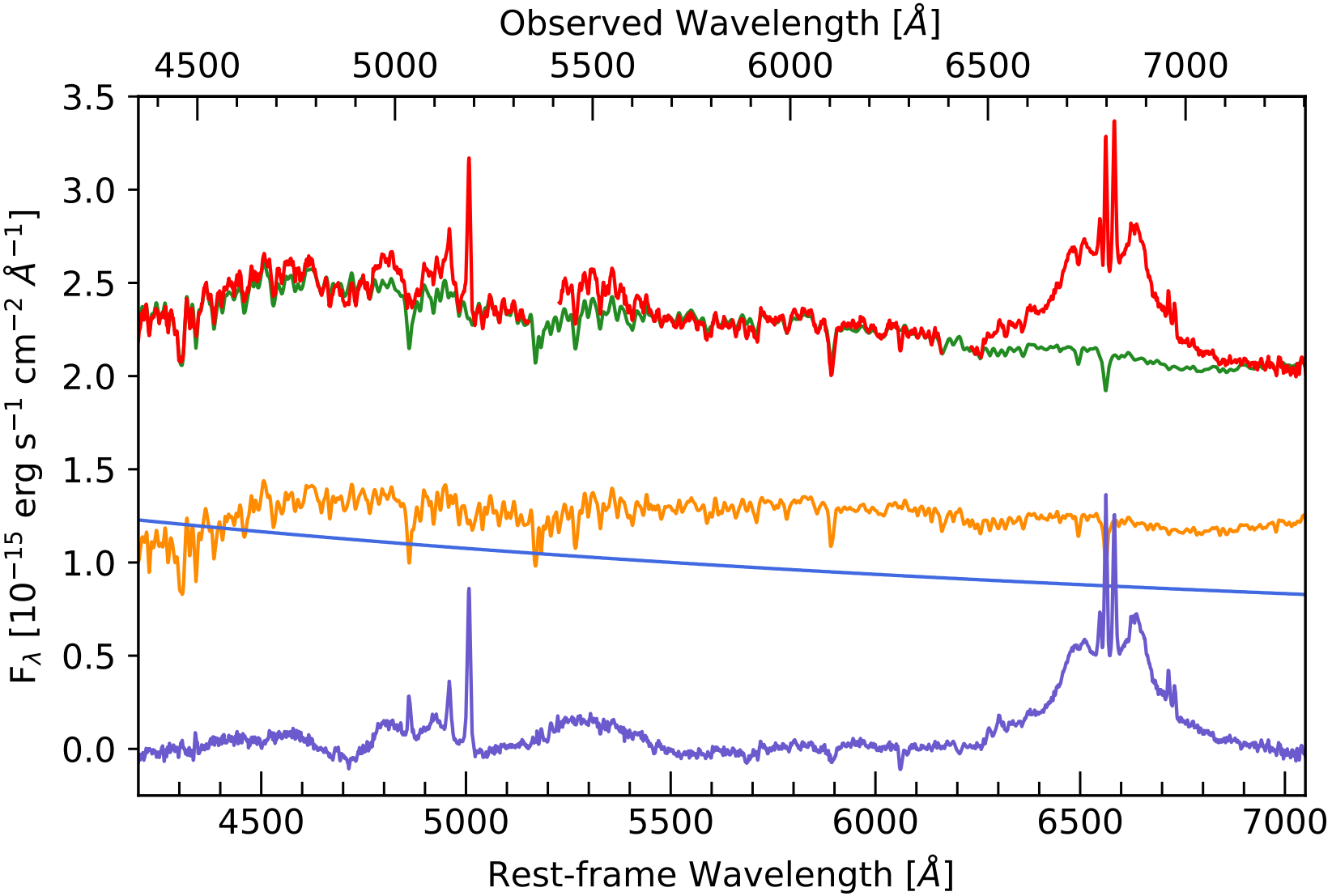

Residuum spectrum of IRAS 23226-3843 from 1991 June 21 indicating the **Balmer absorption component in addition to the emission lines**.

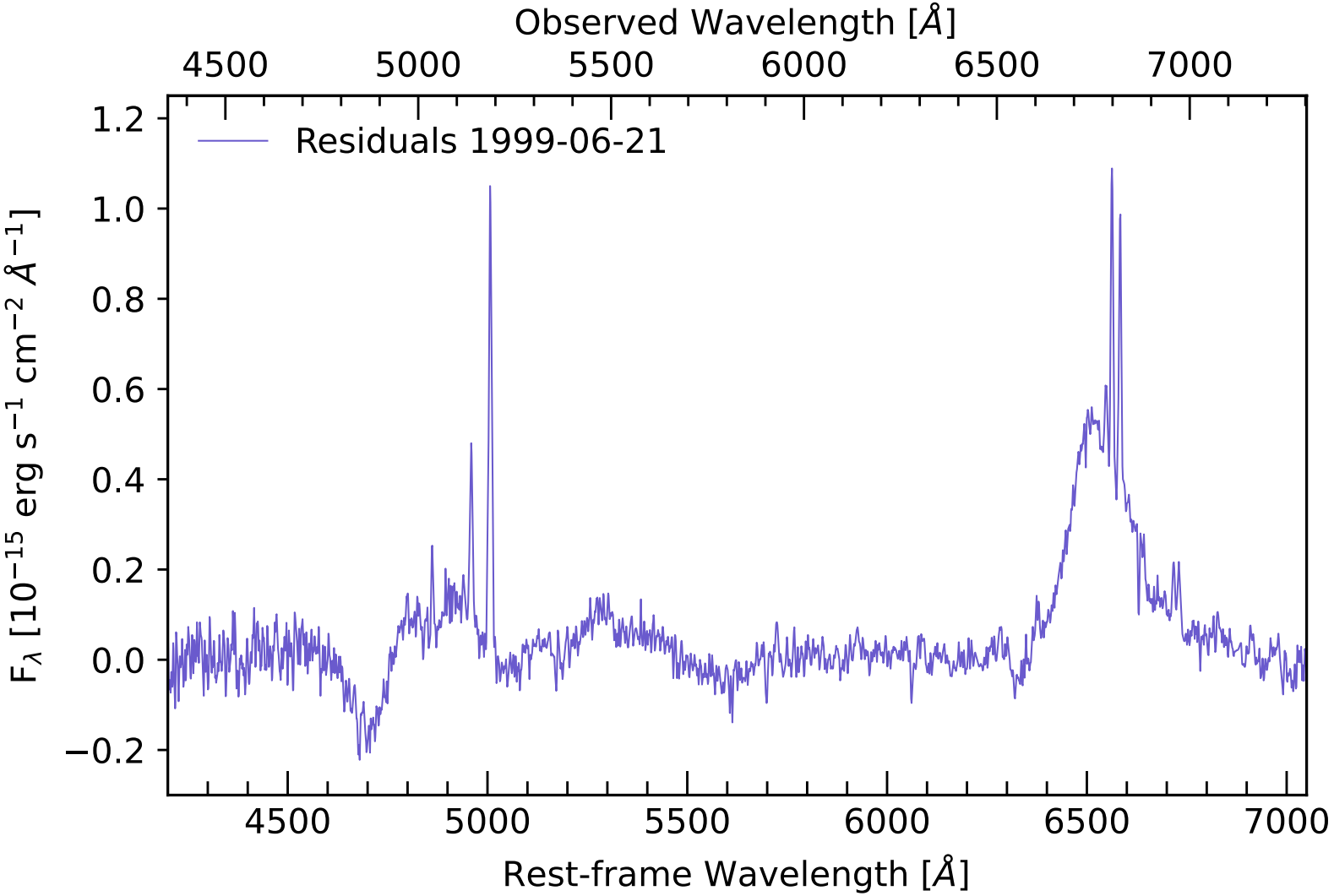

Long-term: SWIFT

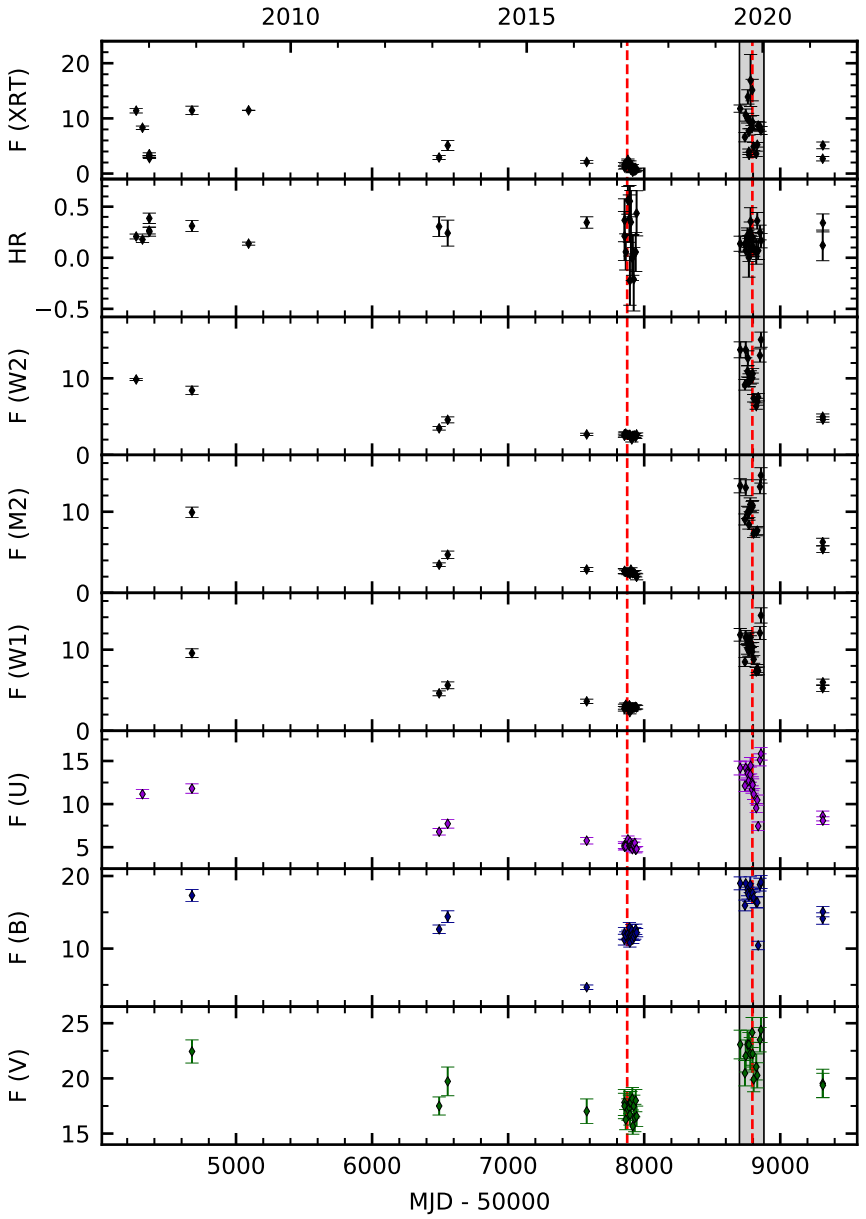

optical lightcurves

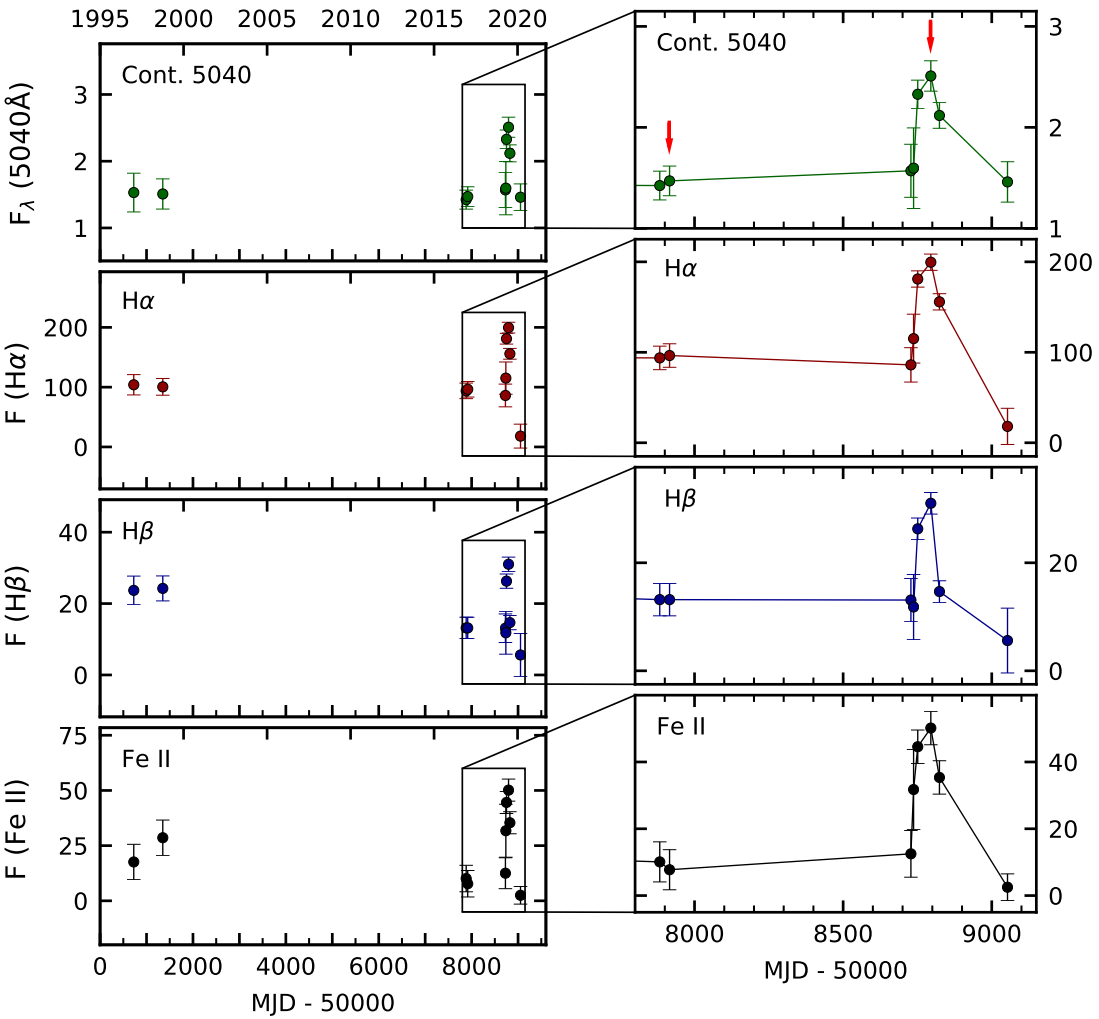

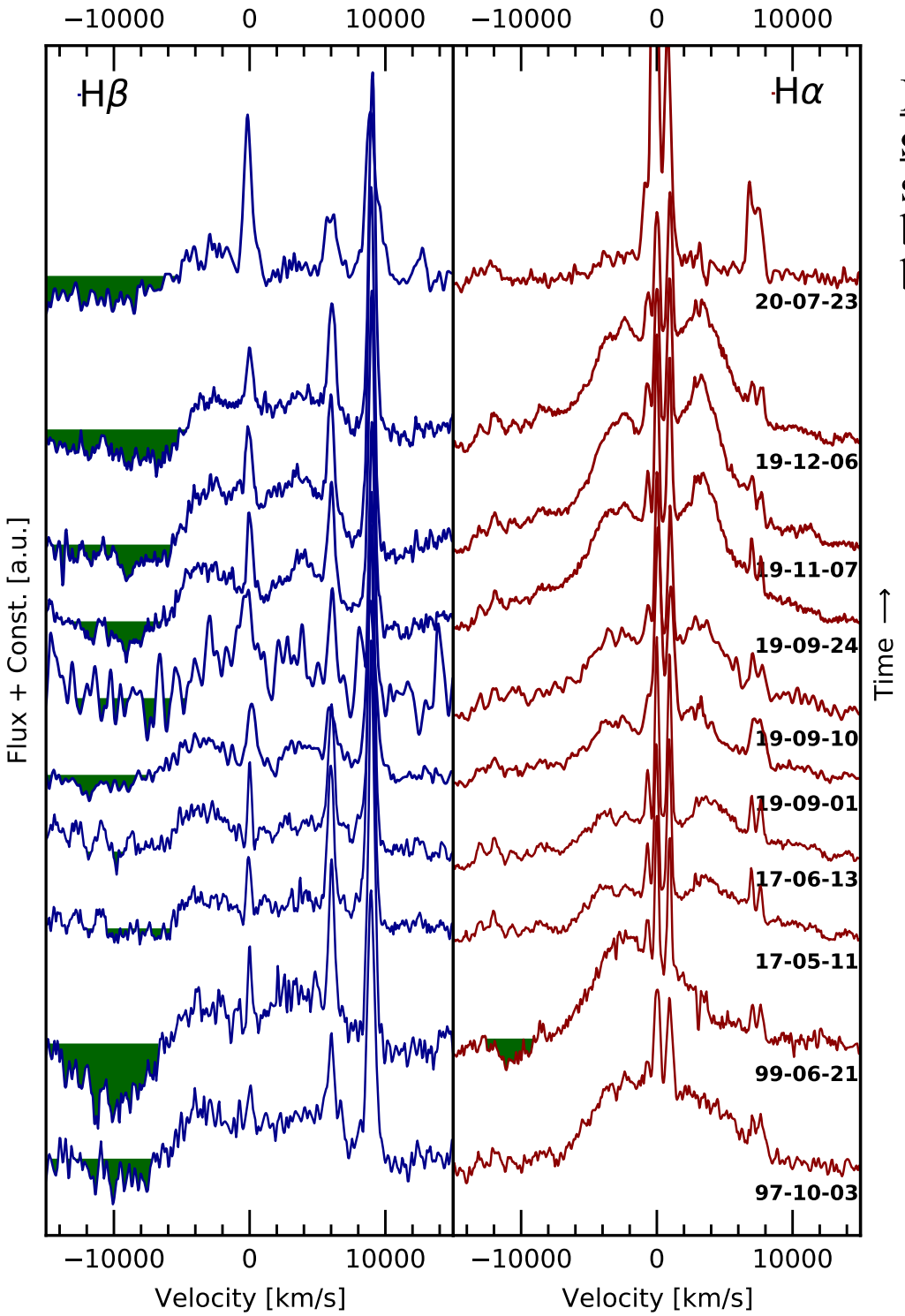

<u>Line profiles of Hα and Hβ in velocity space</u> after subtraction of the host galaxy spectrum. Absorption components in the blue wing of the Balmer lines (i.e., flux below zero) are shaded in green.

2020: Sy2

2019: double peaked Sy1

2017: double peaked Sy1.9

1997/99: single peaked Sy1

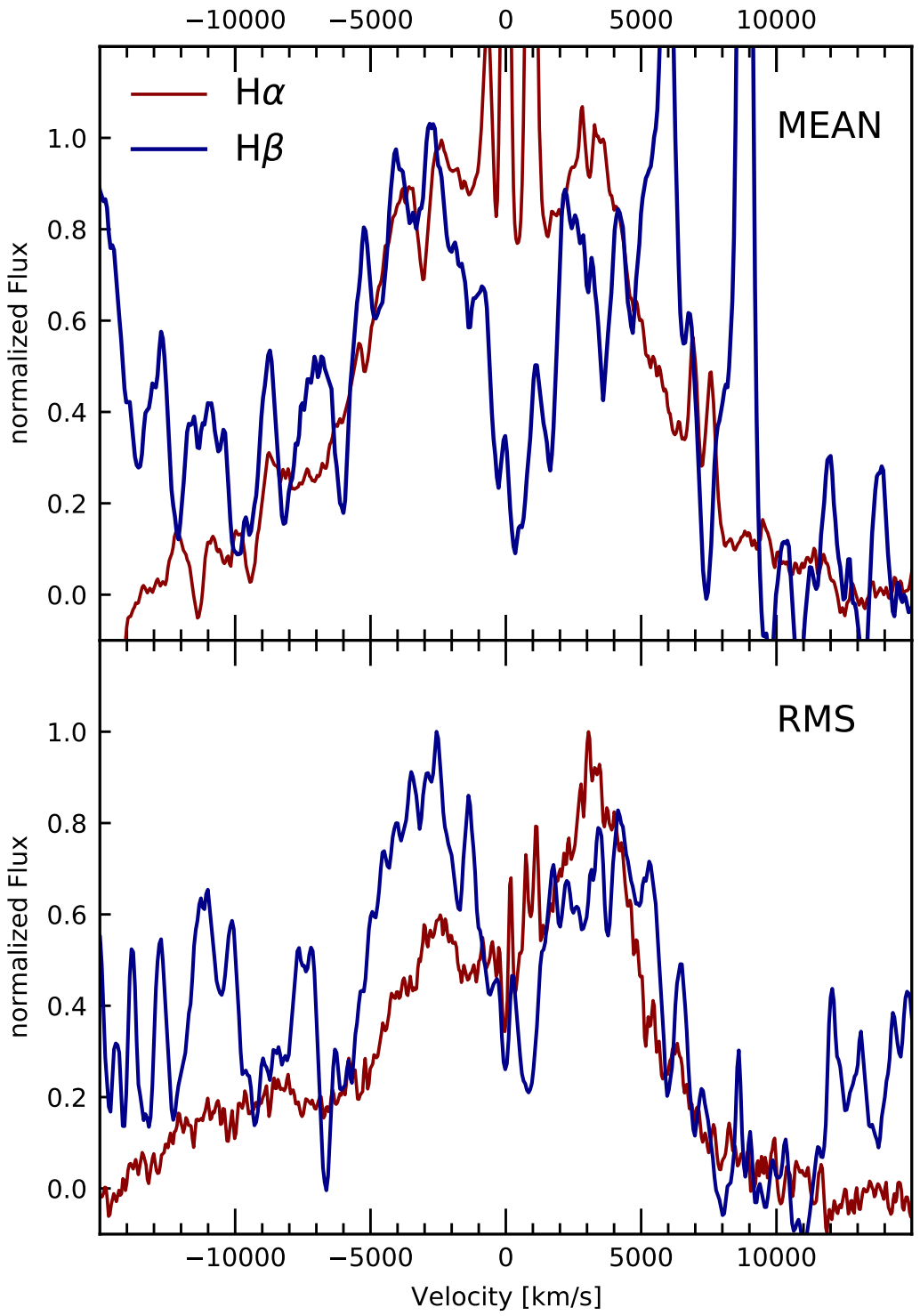

Normalized mean and rms profiles of Hα (red) and Hβ (blue) in velocity space.

Conclusions I

IRAS 23226-3843

- *X-ray variability by factor >30 (2017 - 2020)*
- *X-ray var. by factor 5 within of two months (2020)*

- *opt var. by factor 1.6 within of two months (2020)*
- *opt var. by factor 3 (after correction for hostgalaxy)*

- *X-ray gradient remained constant (SWIFT and XMM spectra)*

- *X-ray spectra featureless + broadened FeK emission*

- *strong line profile changes in very broad Balmer lines:*
  single peaked Sy1 → double peaked Sy1.9 → double peaked Sy1 → Sy2

- *outflow component –10 400 km s^{-1} in Balmer lines*

Conclusions II

IRAS 23226-3843 in comparison to other CL-AGN

	Variability amplitude X-ray	opt. cont.	*spectral type change*
IRAS 23226 (Kollatschny+23)	**>30** *(4y)*	**5** *(2 mon.)* **1.6(3** *w.o. host)* *(2 mon.)*	*Sy1 → Sy2*
HE1136-2304 (Kollatschny+18) (Zetzl+18)	**30** *(24 y)*	**8** *(24y)* **4** *(4y)*	*Sy1.9 → Sy1*
Fairall 9 (Kollatschny+85)		**5** *(6y)*	*Sy1 → Sy1.9*
Mkn1018 (McElroy+16) (Husemann+16)	**8** *(6y)*	**7** *(6y)*	*Sy1 → Sy1.9*
1ES1927+654 (Trakhtenbrot+19) (Ricci+20, Laha+22)	***> 60*** *(1y)*	**> 20** *(1y)*	*Sy2 → Sy1*

X-ray variability: ROSAT All-Sky Survey, XMM-NEWTON Slew Obs.

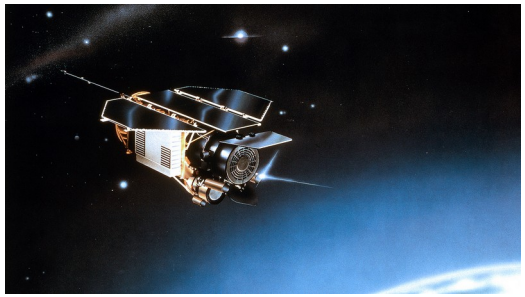

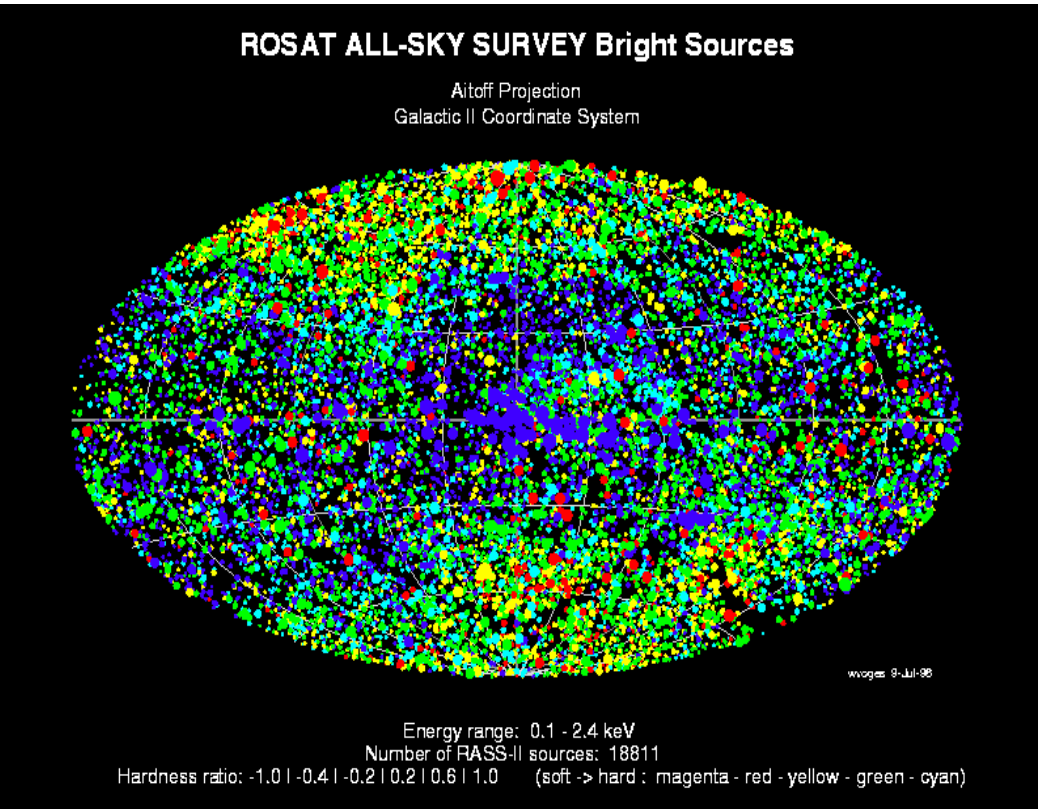

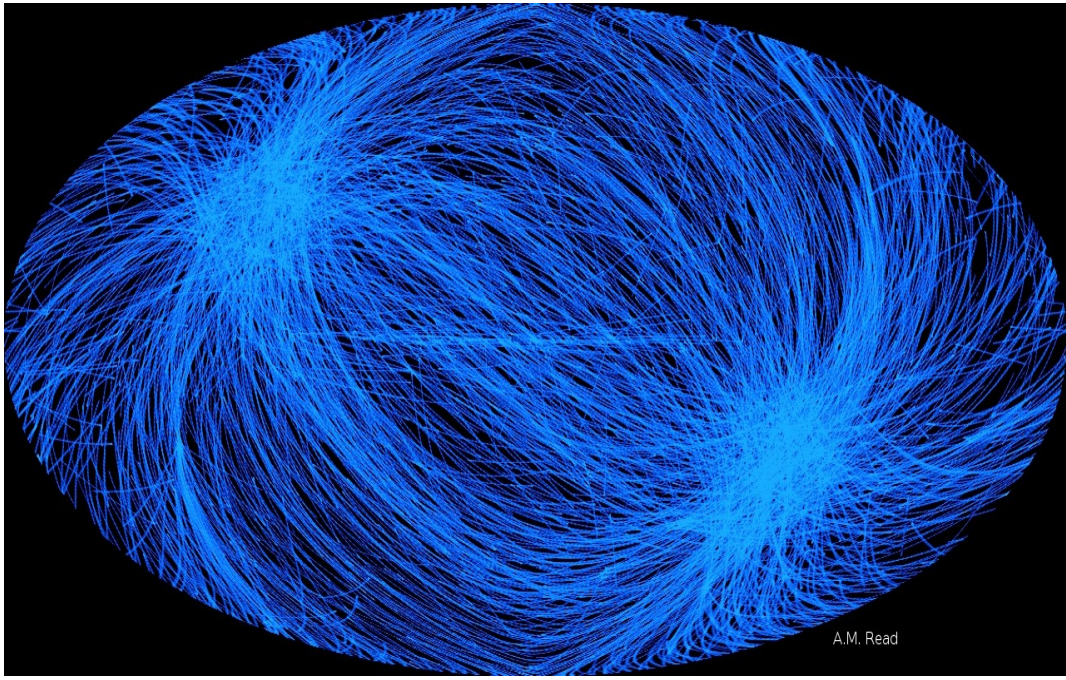

RASS performed 1990/91

- XMM performs slewing maneuvers between targets with the EPIC cameras open
- open-slew speed = 90 deg/hour, i.e. on-source time ~ 14 sec

Changing look AGN program:
- Search for flaring X-ray AGN within XMM Slew Survey: Source flux should be in excess of ± (10 -15) times the flux observed with ROSAT.
- optical changing-look AGN? (type 1 – type 2)

Correlation of XMM-slew survey data with ROSAT

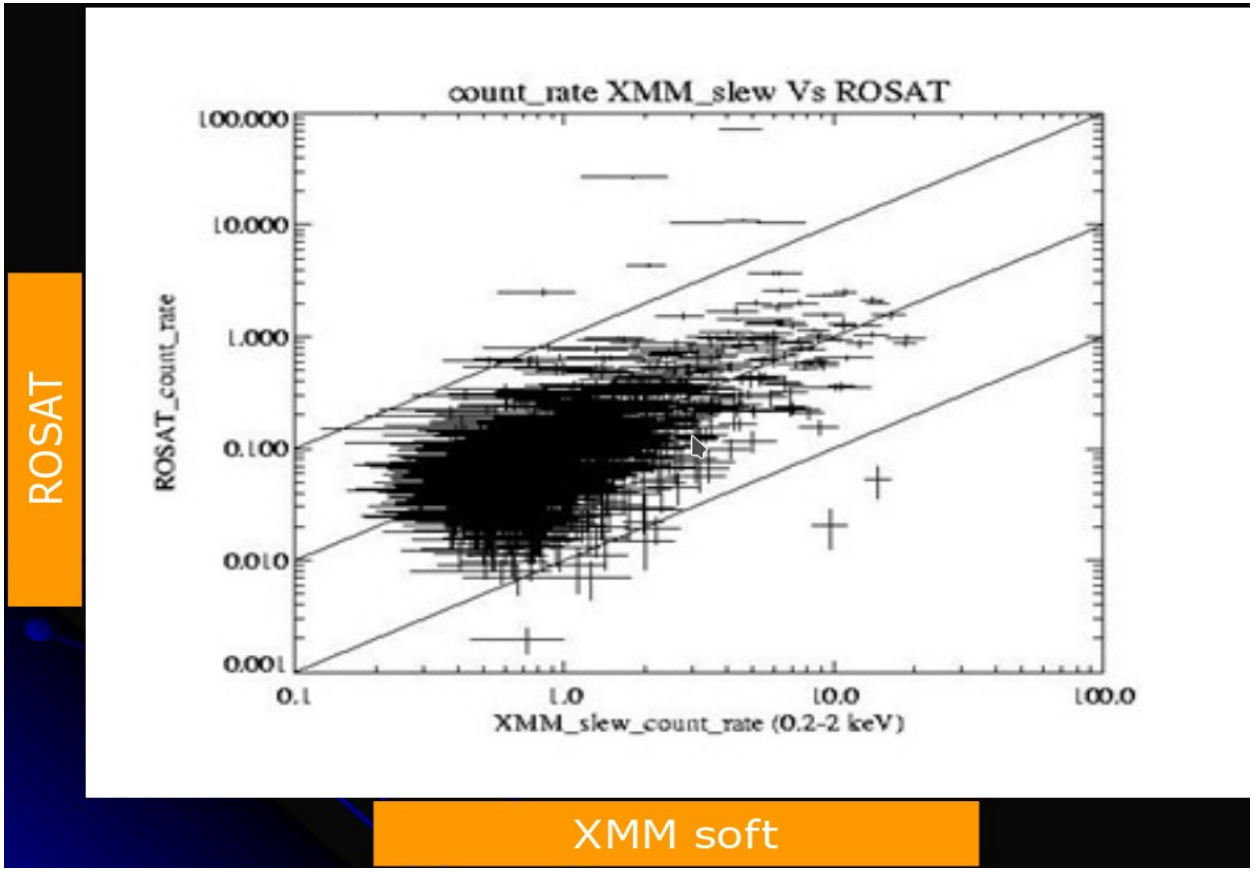

M. Pilar Esquej et al., 2006

Mean XMM/ROSAT count-rate ratio . If deviations > 10: strong X-ray variability

XMM and NuSTAR spectrum of IRAS23226-3843

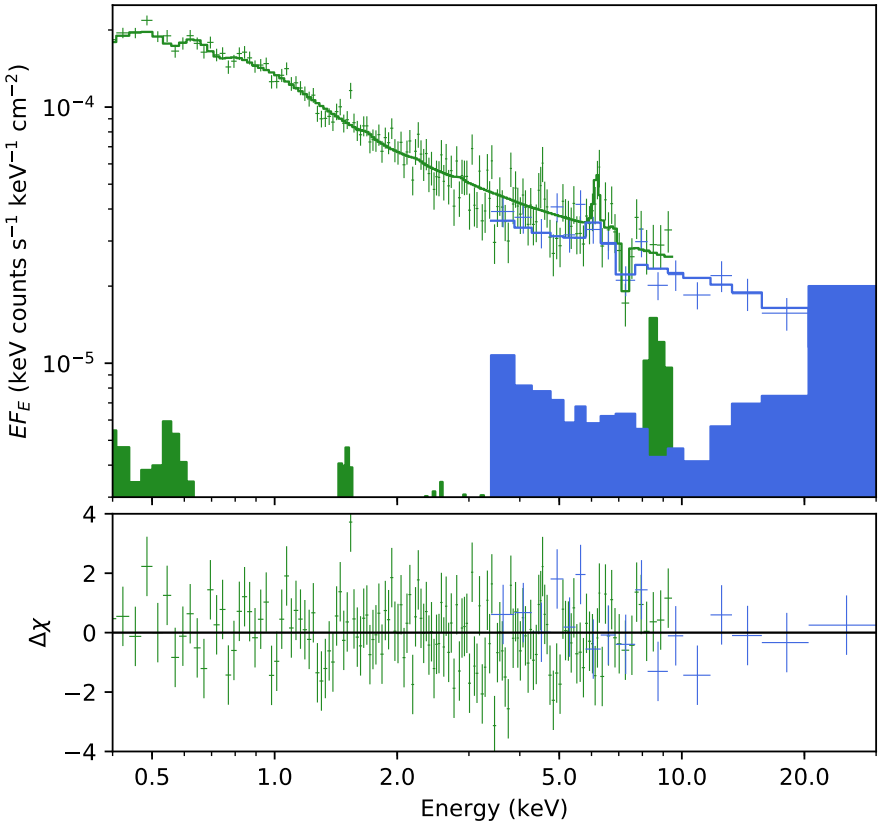

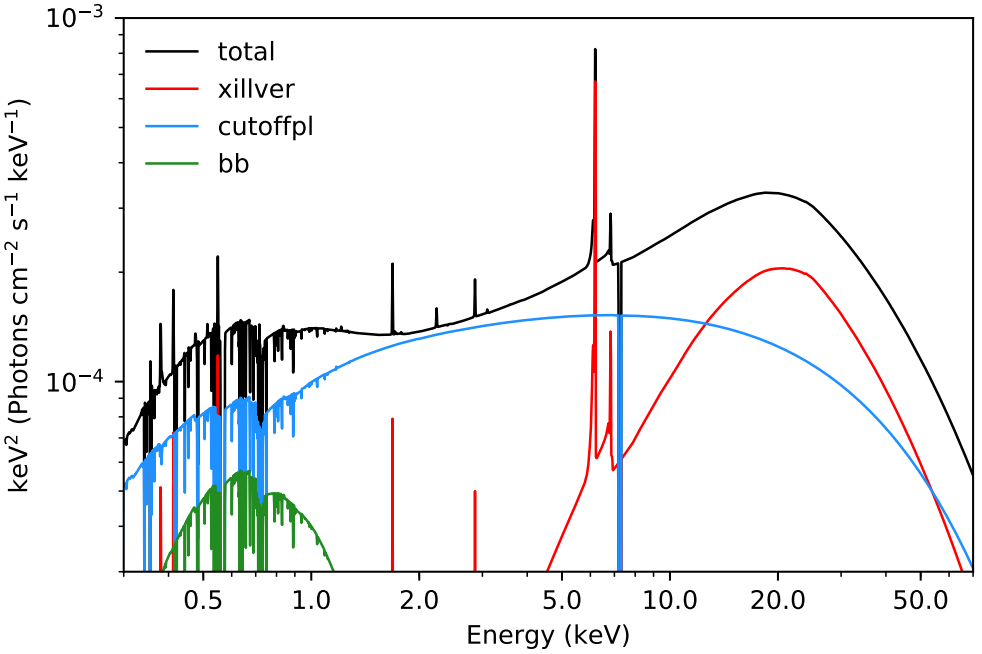

Best-fitting broad-band spectral model, showing different specral components used.